
01 Aug 2014

Communication: Rigorous Quantum Dynamics of O + O₂ Exchange Reactions on an Ab Initio Potential Energy Surface Substantiate the Negative Temperature Dependence of Rate Coefficients

Yaqin Li

Zhigang Sun

Bin Jiang

Daiqian Xie

et. al. For a complete list of authors, see https://scholarsmine.mst.edu/chem_facwork/2131

Follow this and additional works at: https://scholarsmine.mst.edu/chem_facwork

 Part of the [Chemistry Commons](#), and the [Numerical Analysis and Scientific Computing Commons](#)

Recommended Citation

Y. Li et al., "Communication: Rigorous Quantum Dynamics of O + O₂ Exchange Reactions on an Ab Initio Potential Energy Surface Substantiate the Negative Temperature Dependence of Rate Coefficients," *Journal of Chemical Physics*, vol. 141, no. 8, American Institute of Physics (AIP), Aug 2014. The definitive version is available at <https://doi.org/10.1063/1.4894069>

This Article - Journal is brought to you for free and open access by Scholars' Mine. It has been accepted for inclusion in Chemistry Faculty Research & Creative Works by an authorized administrator of Scholars' Mine. This work is protected by U. S. Copyright Law. Unauthorized use including reproduction for redistribution requires the permission of the copyright holder. For more information, please contact scholarsmine@mst.edu.

Communication: Rigorous quantum dynamics of O + O₂ exchange reactions on an *ab initio* potential energy surface substantiate the negative temperature dependence of rate coefficients

Yaqin Li,^{1,2} Zhigang Sun,^{1,2,a)} Bin Jiang,³ Daiqian Xie,⁴ Richard Dawes,^{5,a)} and Hua Guo^{3,a)}

¹State Key Laboratory of Molecular Reaction Dynamics, Dalian Institute of Chemical Physics, Chinese Academy of Sciences, Dalian, Liaoning 116023, China

²Center for Advanced Chemical Physics, University of Science and Technology of China, 96 Jinzhai Road, Hefei 230026, China

³Department of Chemistry and Chemical Biology, University of New Mexico, Albuquerque, New Mexico 87131, USA

⁴Institute of Theoretical and Computational Chemistry, Key Laboratory of Mesoscopic Chemistry, School of Chemistry and Chemical Engineering, Nanjing University, Nanjing 210093, China

⁵Department of Chemistry, Missouri University of Science and Technology, Rolla, Missouri 65409, USA

(Received 23 July 2014; accepted 15 August 2014; published online 26 August 2014)

The kinetics and dynamics of several O + O₂ isotope exchange reactions have been investigated on a recently determined accurate global O₃ potential energy surface using a time-dependent wave packet method. The agreement between calculated and measured rate coefficients is significantly improved over previous work. More importantly, the experimentally observed negative temperature dependence of the rate coefficients is for the first time rigorously reproduced theoretically. This negative temperature dependence can be attributed to the absence in the new potential energy surface of a submerged “reef” structure, which was present in all previous potential energy surfaces. In addition, contributions of rotational excited states of the diatomic reactant further accentuate the negative temperature dependence. © 2014 AIP Publishing LLC. [<http://dx.doi.org/10.1063/1.4894069>]

It has been more than thirty years since the discovery that heavier ozone (O₃) isotopomers are preferentially enriched in the atmosphere.¹ Also found in laboratories,² this so-called mass-independent fractionation (MIF) in the formation of ozone has stimulated much experimental and theoretical work.^{3–6} It is well established that ozone in the atmosphere is produced through the Chapman cycle, in which the metastable O₃* formed by collision between O and O₂ is stabilized by energy loss to a third collision partner. While a complete explanation of the strong and surprising isotope effect has not been achieved yet,⁷ it is reasonably certain that it has a quantum mechanical origin associated with the zero-point energy differences among various O₂ isotopomers.⁸

A closely related isotope effect has also been observed for the O + O₂ isotope exchange reactions,⁹ which competes with the formation of O₃. Interestingly, the rate coefficients of the exchange reactions have been found to possess a negative temperature dependence,^{10,11} signifying the absence of a reaction barrier. However, this negative temperature dependence has been notoriously difficult to reproduce theoretically,^{11–14} despite the fact that the potential energy surfaces (PESs) used in previous calculations are barrierless.^{15,16} In an insightful study, Schinke and co-workers^{11,12} pointed out that the temperature dependence of the exchange rate coefficients is sensitive to a submerged “reef”-like feature in the O + O₂ entrance (and exit) chan-

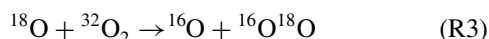
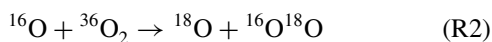
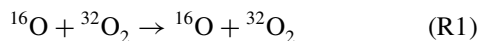
nel of the O₃ PES, which has been found in most of previous *ab initio* calculations.^{17–20} They showed that if the PES was adjusted to remove the “reef,” interestingly, the calculated rate coefficients then took on a negative temperature dependence and agreed better with experiment.¹²

We have attempted to resolve this controversy by mapping out the ozone formation PES with high-level *ab initio* approaches. It has recently been shown by Dawes *et al.*^{21,22} that the “reef”-like saddle point present in many previous ozone PESs is an artifact of the electronic structure model used to generate the PESs. The new Dawes-Lolur-Li-Jiang-Guo (DLLJG) PES, obtained with a dynamically weighted^{23,24} explicitly-correlated multi-reference configuration interaction^{25–27} approach with the Davidson correction²⁸ and spin-orbit correction (DW-MRCI-F12+Q), is “reef”-free, thus qualitatively different from all previous ozone PESs.^{16,20,29} The disappearance of the “reef” structure essentially results from the employment of a large basis set, larger active configuration spaces, and dynamical weighting of excited states. Further evidence for the absence of a reef was provided by Tyuterev *et al.*, who found improved agreement with experiment for the highest lying known vibrational levels when a “Dawes correction” to remove the reef was applied to their PES.²⁹ In our recent work, quantum statistical model (QSM) calculations on the DLLJG PES have already produced a negative temperature dependence for the O + O₂ rate coefficients.²² However, this QSM-based conclusion is tentative as the O + O₂ exchange reactions are known to have a strong non-statistical character,^{30–32} which prevents an

^{a)}Authors to whom correspondence should be addressed. Electronic addresses: zsun@dicp.ac.cn; dawesr@mst.edu; and hguo@unm.edu

accurate description of the kinetics with any form of statistical theory. To provide a conclusive assessment of the DLLJG PES, we report here an extensive quantum dynamics investigation, which computes the rate coefficients and their temperature dependence from state-to-state and initial-state selected integral cross sections.

Our quantum scattering calculations focused on the following exchange reactions:



The state-to-state calculations, which employed a reactant Jacobi coordinate-based quantum wave packet method,³³ minimize the errors at low collision energies due to the incomplete absorption of the wave packet in asymptotes. The wave packet was propagated using an efficient high-order split operator method,³⁴ which allows a large time step of 120 a.u. The PES used in the calculation is that of Dawes *et al.*,²² which includes an analytical form developed by Lepers *et al.*³⁵ to better describe the asymptotic regions. An absorbing potential was applied at the end of both R and r grids to impose outgoing boundary conditions. All partial waves up to $J = 94$ were included. More details of the quantum scattering calculations and the associated parameters are found in the supplementary material.³⁶

The state-to-state integral cross section (ICS) at collision energy E_c was obtained from the S-matrix element $S_{v_f j_f K_f \leftarrow v_i j_i K_i}^J$ as follows:

$$\begin{aligned} \sigma_{v_f j_f \leftarrow v_i j_i}(E_c) &= \frac{\pi}{(2j_i + 1)\kappa_{v_i j_i}^2} \sum_{K_f} \sum_{K_i} \sum_J (2J + 1) |S_{v_f j_f K_f \leftarrow v_i j_i K_i}^J|^2, \end{aligned} \quad (1)$$

where the wavevector is defined as $\kappa_{v_i j_i} = \sqrt{2\mu E_c}$ with μ as the translational reduced mass. All necessary helicity channels, up to $2J/3$, labeled by the projection of the total angular momentum J on the body-fixed axis (K), were included.³¹

The initial state-specified thermal rate coefficients were obtained by Boltzmann averaging their ICSs:

$$k_{v_i j_i}(T) = Q_{el}^{-1} \sqrt{\frac{8}{\pi\mu(k_B T)^3}} \int_0^\infty \sigma_{v_i j_i}(E_c) e^{-E_c/k_B T} E_c dE_c, \quad (2)$$

where k_B and T are the Boltzmann constant and temperature in Kelvin, respectively. Q_{el} is the electronic partition function for the exchange reaction, which is given by³⁷

$$Q_{el} = 3[5 + 3e^{-227.6/T} + e^{-325.9/T}]. \quad (3)$$

The thermal averaged rate coefficient $k(T)$ can then be obtained by a Boltzmann average over the initial ro-vibrational

states:

$$k(T) = \sum_{v_i j_i} \frac{(2j_i + 1)e^{-E_{v_i j_i}/k_B T}}{Q_{v_i j_i}} k_{v_i j_i}(T), \quad (4)$$

where $E_{v_i j_i}$ and $Q_{v_i j_i}$ are the reactant ro-vibrational energies and corresponding partition functions, respectively.

Since ^{18}O and ^{16}O have $I = 0$ nuclear spin, there are no even rotational states for $^{32}\text{O}_2$ and $^{36}\text{O}_2$, because of nuclear spin statistics.³⁸ As a result, only odd initial rotational states of the reactants (j_i) for R1, R2, and R3 should be considered. However, the number of initial wave packets needed is proportional to $2j_i + 1$. To minimize the computational costs in state-to-state calculations, we evaluated a strategy of using the (forbidden) $j_i = 0$ initial state to obtain the cross sections and the initial state-specified rate coefficients for these reactions. This approximation is reasonable as O_2 has a large moment of inertia, and the initial rotational level typically has little impact on reactivity of complex-forming reactions, at least for the lowest few rotational states.³⁹ As shown in the supplementary material,³⁶ the total reaction probabilities and ICSs for $j_i = 0$ and 1 are almost identical for R1. As a result, all state-to-state quantum calculations reported below for R2 and R1 used the $j_i = 0$ ro-vibrational state of the O_2 reactants. The effects of higher j_i states were investigated for R3 with selected initial states of $(v_i j_i) = (0, 5)$, $(0, 9)$, and $(0, 21)$. The ICSs of other reactant rotational states were obtained by interpolating those of the three initial rovibrational states, according to the following equation:

$$\sigma_{v_i j_i}(E_c) = \frac{E_{j_i} - E_{j_s}}{E_{j_s} - E_{j_l}} \sigma_{v_i j_l}(E_c) + \frac{E_{j_l} - E_{j_i}}{E_{j_s} - E_{j_l}} \sigma_{v_i j_s}(E_c), \quad (5)$$

where j_l and j_s are the rotational quantum number larger (l) or smaller (s) than j_i , respectively. On the other hand, the effect of vibrationally excited O_2 is negligible as its vibrational frequency is about 0.19 eV. Finally, we note that the nuclear spin statistics of the product such as $^{32}\text{O}_2$ was not explicitly considered either, since it hardly affects the total integral cross sections and rate coefficients, as argued using the state-to-state results in the supplementary material.³⁶

The calculated integral cross sections ($\sigma(E_c)$) for R1, R2, and R3 with $j_i = 0$ are presented in the upper panel of Figure 1 as a function of collision energy. It is clear that these excitation functions decay monotonically at low collision energies, consistent with the barrierless reaction pathway. This behavior is drastically different from the excitation functions computed on older PESs with a ‘‘reef’’ structure, where the ICS typically increases with E_c .^{11,13,14} Significant isotope effects are also apparent: R2 has the smallest reactivity, followed by R3, while R1 is most reactive. This ordering is intriguing as R1 is thermoneutral and symmetric with respect to the exchange of the three oxygen atoms, while R2 and R3 are endothermic and exothermic, respectively. Some oscillations are present in the excitation functions, which presumably stem from resonances near the reaction threshold. The analysis of these resonances, which are relevant to MIF in ozone formation, will be presented in a future publication.

In the lower panel of Figure 1, the ICSs of R3 for rotational states $j_i = 1, 3, \dots, 21$ are displayed. It is observed that

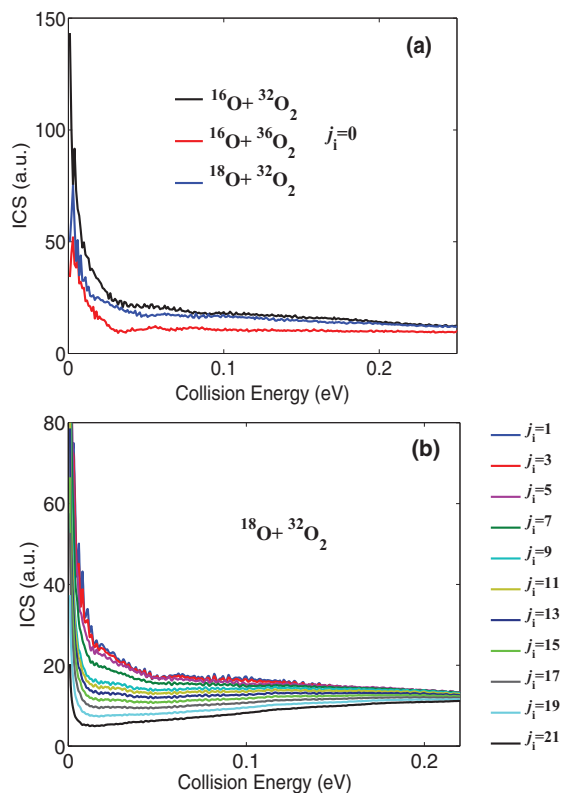


FIG. 1. (a) Comparison of initial state specified total integral cross sections of R1 (black), R2 (red), and R3 (blue). (b) Comparison of total integral cross sections with different initial rotational states of R3 obtained on the DLLJG PES.²²

at low collision energies, the ICS decreases with the increasing rotational quantum number of the initial state. As a result, contributions from rotationally excited O_2 should be included in computing the thermal rate coefficients.

In the upper panel of Figure 2, the rate coefficients of R1, R2, and R3 with the ground ro-vibrational state ($j_i = 0$) are presented as a function of temperature. Also plotted in the same figure are the rate coefficients with $j_i = 0$ calculated on the modified Siebert-Schinke-Bittererova (SSB) PES of Babikov *et al.*^{15,16} It is clear that rate coefficients on the SSB PES are significantly smaller than those obtained on the DLLJG PES. More importantly, the negative temperature dependence of the calculated rate coefficients on the DLLJG PES is apparent, while a slightly positive temperature dependence was found for the rate coefficients calculated using the SSB PES. This can be readily understood as the “reef” structure in the modified SSB PES serves as a bottleneck and lower the reactivity.³¹

In the lower panel of Figure 2, the R3 rate coefficients including all allowed reactant rotational states up to $j_i = 21$ are displayed. In the temperature range shown, it is observed that the rate coefficient decreases with the increasing rotational quantum number. As a result, the inclusion of higher rotational states of the reactant steepens the negative temperature dependence of $k(T)$. This conclusion is also confirmed with quasi-classical trajectory calculations in the supplementary material.³⁶

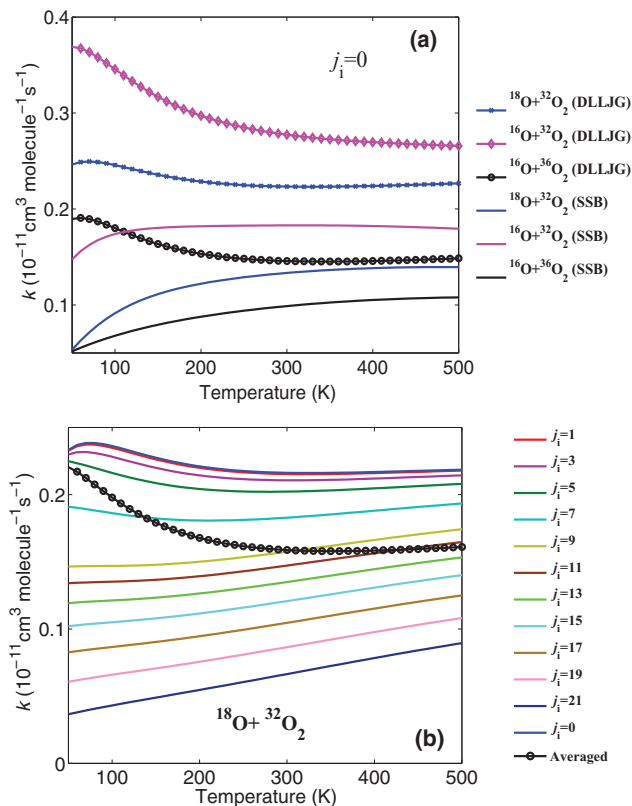


FIG. 2. (a) Comparison of initial state specified with $j_i = 0$ rate coefficients of R1, R2, and R3 obtained on the DLLJG²² and modified SSB^{15,16} PESs. (b) Comparison of initial state specified rate coefficients and thermal averaged rate coefficients of R3 obtained on the DLLJG PES.²²

In order to compare with experiment, we have empirically corrected the thermal rate coefficients of R1 and R2 with $j_i = 0$, using the scaling factor between $k(T)$ and $k_{v,j_i=0}(T)$ for R3. The resulting rate coefficients for all three reactions are shown in Figure 3, along with the available experimental results. The negative temperature dependence of the calculated rate coefficients for all three reactions is apparent, although the agreement with experimental data is still imperfect. We also note that the rate coefficients obtained on the DLLJG PES are in much better agreement with the experimental values than those on the SSB PES, further suggesting the improved accuracy of the new PES. In addition, the calculated kinetic isotope effect (k_3/k_2) at 300 K is 1.53, which is in line with the experimental value of 1.27.^{9,11} The successful reproduction of the experimentally observed negative temperature dependence for all three isotope exchange reactions using a dynamically exact quantum method provides the strongest evidence to date in support of the global accuracy of the DLLJG PES, validating the absence of the “reef” structure in the entrance and exit channels of the PES.

The remaining discrepancy with experiment may have several possible origins. First, there may still be inaccuracies in the PES, due to internal contraction⁴⁰ and high-order electron correlation. Second, there might be non-adiabatic interactions in the asymptotic region amongst the 27 electronic states that are coupled by spin-orbit couplings,^{35,41} although a 2D study mentioned in our previous investigation predicted

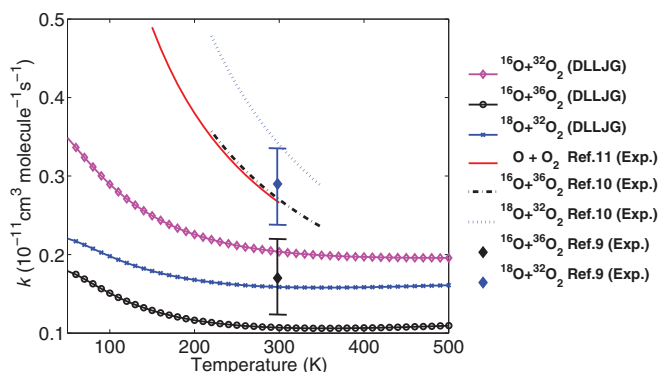


FIG. 3. Comparison of thermal rate coefficients of R1, R2, and R3 obtained on the DLLJG PES.²² The available experimental data are also presented for comparison.

this to be negligible.²¹ At the same time, there are large experimental uncertainties in the measured rate coefficients.

To summarize, an extensive quantum wavepacket study has been carried out for several O + O₂ isotope exchange reactions on the most dynamically accurate global ozone PES to date. The calculated thermal rate coefficients are in much better agreement with experiment than those obtained previously on less accurate PESs. Perhaps most significantly, the experimentally observed negative temperature dependence of these rate coefficients is reproduced, which can be mostly attributed to the absence of a “reef” structure on the new PES, accentuated by the excited reactant rotational states.

Because the accuracy of PESs is a pre-requisite for accurate quantum dynamical calculations, errors in the PES could lead to false dynamical predictions. There is a large body of dynamical calculations based on the existence of such a “reef” structure in the ozone PES, including some on the MIF of ozone formation.^{42–46} As a result, the impact of the artificial “reef” structure in earlier PESs on these dynamical calculations needs to be carefully reassessed. Our new PES is expected to provide a much more reliable platform for understanding both the bimolecular exchange reaction and unimolecular ozone forming reaction, which holds the key to the ultimate elucidation of the ozone MIF.

This work was supported by the Natural Science Foundation of China (Grant Nos. 21222308, 21103187, and 21133006 to Z.S.), National Natural Science Foundation of China (21133006 and 21273104 to D.X.) and the Chinese Ministry of Science and Technology (2013CB834601 to D.X.), National Science Foundation (CHE-1300945 to R.D.), and NASA (11-EXO11-0107 to H.G.). We thank Beatrice Bussery-Honvault for sending us her asymptotic potential for O + O₂.

¹K. Mauersberger, *Geophys. Res. Lett.* **8**, 935, doi:10.1029/GL008i008p00935 (1981).

²M. H. Thiemens and J. E. Heidenreich III, *Science* **219**, 1073 (1983).

³K. Mauersberger, D. Krankowski, C. Janssen, and R. Schinke, *Adv. At. Mol. Opt. Phys.* **50**, 1 (2005).

⁴R. Schinke, S. Y. Grebenshchikov, M. V. Ivanov, and P. Fleurat-Lessard, *Annu. Rev. Phys. Chem.* **57**, 625 (2006).

⁵M. H. Thiemens, *Annu. Rev. Earth Planet. Sci.* **34**, 217 (2006).

⁶R. A. Marcus, *Adv. Quantum Chem.* **55**, 5 (2008).

⁷R. A. Marcus, *Proc. Natl. Acad. Sci. U.S.A.* **110**, 17703 (2013).

⁸C. Janssen, J. Guenther, K. Mauersberger, and D. Krankowski, *Phys. Chem. Chem. Phys.* **3**, 4718 (2001).

⁹S. M. Anderson, F. S. Klein, and F. Kaufman, *J. Chem. Phys.* **83**, 1648 (1985).

¹⁰M. R. Wiegell, N. W. Larsen, T. Pedersen, and H. Egsgaard, *Int. J. Chem. Kinet.* **29**, 745 (1997).

¹¹P. Fleurat-Lessard, S. Y. Grebenshchikov, R. Schinke, C. Janssen, and D. Krankowski, *J. Chem. Phys.* **119**, 4700 (2003).

¹²P. Fleurat-Lessard, S. Y. Grebenshchikov, R. Siebert, R. Schinke, and N. Halberstadt, *J. Chem. Phys.* **118**, 610 (2003).

¹³K.-L. Yeh, D. Xie, D. H. Zhang, S.-Y. Lee, and R. Schinke, *J. Phys. Chem. A* **107**, 7215 (2003).

¹⁴S. Y. Lin and H. Guo, *J. Phys. Chem. A* **110**, 5305 (2006).

¹⁵R. Siebert, R. Schinke, and M. Bittererova, *Phys. Chem. Chem. Phys.* **3**, 1795 (2001).

¹⁶D. Babikov, B. K. Kendrick, R. B. Walker, R. T. Pack, P. Fleurat-Lessard, and R. Schinke, *J. Chem. Phys.* **118**, 6298 (2003).

¹⁷R. Hernandez-Lamonedá, M. R. Salazar, and R. T. Pack, *Chem. Phys. Lett.* **355**, 478 (2002).

¹⁸R. Schinke and P. Fleurat-Lessard, *J. Chem. Phys.* **121**, 5789 (2004).

¹⁹F. Holka, P. G. Szalay, T. Muller, and V. G. Tyuterev, *J. Phys. Chem. A* **114**, 9927 (2010).

²⁰M. Ayouz and D. Babikov, *J. Chem. Phys.* **138**, 164311 (2013).

²¹R. Dawes, P. Lolur, J. Ma, and H. Guo, *J. Chem. Phys.* **135**, 081102 (2011).

²²R. Dawes, P. Lolur, A. Li, B. Jiang, and H. Guo, *J. Chem. Phys.* **139**, 201103 (2013).

²³M. P. Deskevich, D. J. Nesbitt, and H.-J. Werner, *J. Chem. Phys.* **120**, 7281 (2004).

²⁴R. Dawes, A. W. Jasper, C. Tao, C. Richmond, C. Mukarakate, S. H. Kable, and S. A. Reid, *J. Phys. Chem. Lett.* **1**, 641 (2010).

²⁵H.-J. Werner, *Adv. Chem. Phys.* **69**, 1 (1987).

²⁶T. Shiozaki, G. Knizia, and H.-J. Werner, *J. Chem. Phys.* **134**, 034113 (2011).

²⁷T. Shiozaki and H.-J. Werner, *Mol. Phys.* **111**, 607 (2013).

²⁸S. R. Langhoff and E. R. Davidson, *Int. J. Quantum Chem.* **8**, 61 (1974).

²⁹V. G. Tyuterev, R. V. Kochanov, S. A. Tashkun, F. Holka, and P. G. Szalay, *J. Chem. Phys.* **139**, 134307 (2013).

³⁰A. L. Van Wyngarden, K. A. Mar, K. A. Boering, J. J. Lin, Y. T. Lee, S.-Y. Lin, H. Guo, and G. Lendvay, *J. Am. Chem. Soc.* **129**, 2866 (2007).

³¹Z. Sun, L. Liu, S. Y. Lin, R. Schinke, H. Guo, and D. H. Zhang, *Proc. Natl. Acad. Sci. U.S.A.* **107**, 555 (2010).

³²A. L. Van Wyngarden, K. A. Mar, J. Quach, A. P. Q. Nguyen, A. A. Wiegell, S.-Y. Lin, G. Lendvay, H. Guo, J. J. Lin, Y. T. Lee, and K. A. Boering, *J. Chem. Phys.* **141**, 064311 (2014).

³³Z. Sun, X. Lin, S.-Y. Lee, and D. H. Zhang, *J. Phys. Chem. A* **113**, 4145 (2009).

³⁴Z. Sun, W. Yang, and D. H. Zhang, *Phys. Chem. Chem. Phys.* **14**, 1827 (2012).

³⁵M. Lepers, B. Bussery-Honvault, and O. Dulieu, *J. Chem. Phys.* **137**, 234305 (2012).

³⁶See supplementary material at <http://dx.doi.org/10.1063/1.4894069> for a detailed description of the quantum and quasi-classical trajectory calculations and additional results.

³⁷A. Gross and G. D. Billing, *Chem. Phys.* **217**, 1 (1997).

³⁸P. R. Bunker and P. Jensen, *Molecular Symmetry and Spectroscopy* (NRC Research Press, Ottawa, 1998).

³⁹H. Guo, *Int. Rev. Phys. Chem.* **31**, 1 (2012).

⁴⁰L. Harding, S. Klippenstein, H. Lischka, and R. Shepard, *Theor. Chem. Acc.* **133**, 1429 (2013).

⁴¹M. Tashiro and R. Schinke, *J. Chem. Phys.* **119**, 10186 (2003).

⁴²D. Babikov, B. K. Kendrick, R. B. Walker, R. T. Pack, P. Fleurat-Lessard, and R. Schinke, *J. Chem. Phys.* **119**, 2577 (2003).

⁴³T. Xie and J. M. Bowman, *Chem. Phys. Lett.* **412**, 131 (2005).

⁴⁴R. Schinke and P. Fleurat-Lessard, *J. Chem. Phys.* **122**, 094317 (2005).

⁴⁵S. Y. Grebenshchikov and R. Schinke, *J. Chem. Phys.* **131**, 181103 (2009).

⁴⁶M. V. Ivanov and D. Babikov, *Proc. Natl. Acad. Sci. U.S.A.* **110**, 17708 (2013).